



AUSTRALIAN JOURNAL OF BASIC AND APPLIED SCIENCES

ISSN:1991-8178 EISSN: 2309-8414
Journal home page: www.ajbasweb.com



Achieving the Target Crystal Size Distribution in the Case of Agglomeration and Breakage for Batch Cooling Crystallization Process

¹Zakirah Mohd Zahari, ²Suriyati Salleh, ³Noor Asma Fazli Abdul Samad

Universiti Malaysia Pahang, Faculty of Chemical and Natural Resources Engineering, , 26300, Gambang, Pahang, Malaysia.

Address For Correspondence:

Noor Asma Fazli Abdul Samad, Universiti Malaysia Pahang, Faculty of Chemical and Natural Resources Engineering, 26300, Gambang, Pahang. Email: asmafazli@ump.edu.my

ARTICLE INFO

Article history:

Received 18 September 2016

Accepted 21 January 2017

Available online 26 January 2017

Keywords:

Crystal Size Distribution, Supersaturation, Analytical Estimator, Agglomeration, Breakage.

ABSTRACT

This paper aims to study the effects of agglomeration and breakage phenomena on the target crystal size distribution (CSD) in batch cooling crystallization process. An analytical CSD estimator has been extended to cover the effects of agglomeration and breakage in order to obtain the set-point trajectory needed for achieving the desired CSD. This set-point provides the supersaturation limit and total crystallization time that need to be maintained throughout the operation in order to achieve the target CSD. The application of the extended analytical CSD estimator is highlighted through sucrose case study where three different set-points generated from analytical CSD estimator is tested to achieve a similar crystal size distribution. In addition the performance of the controller for maintaining the crystallization operation is also discussed.

INTRODUCTION

Crystallization is an important separation process due to its ability to produce a highly purity separation product. Usually, the process can be operated in the continuous and batch modes. However, a batch crystallization process are widely used in many chemical, pharmaceutical, food and manufacturing industries rather than continuous due to its ability to produce a narrow crystal size distribution (CSD) and a large mean of a crystal product which contributing to high purity crystalline product (Paengjuntuek *et al.*, 2008). The main specifications of the crystal product are usually given in terms of crystal size, size distribution, shape and purity (Samad *et al.*, 2013). In order to obtain the desired quality of crystal product, it is necessary to control the crystallization operation within the metastable region. Usually a supersaturation set-point control is one of the ways to control the distribution of crystal particles in the batch cooling crystallization process. Here the set-point that needs to be maintained for the controller purpose can be generated using analytical CSD estimator (Samad *et al.*, 2013; Nagy and Aamir, 2012).

The analytical CSD estimator is developed based on the assumptions of constant supersaturation throughout the entire batch operation in the absence of nucleation (Nagy and Aamir, 2012). The function of this estimator is to generate a supersaturation set-point that can provide a desired target CSD based on the specified initial seed distribution and known growth kinetics (Samad *et al.*, 2013). The generated set-point represents the supersaturation value that needs to be maintained using a proper controller during the entire batch operation in order to achieve the desired target CSD. However the effects of agglomeration and breakage are neglected in current analytical CSD estimator. Both phenomena usually affecting the final CSD of the crystal product because the crystal particles tend to merge with other crystal particles due to the stirring in the crystallization operation and may also break because of the collision between particles. Therefore, the aim of this study is to

Open Access Journal

Published BY AENSI Publication

© 2017 AENSI Publisher All rights reserved

This work is licensed under the Creative Commons Attribution International License (CC BY).

<http://creativecommons.org/licenses/by/4.0/>



Open Access

To Cite This Article: Zakirah Mohd Zahari, Suriyati Salleh, Noor Asma Fazli Abdul Samad., Achieving the Target Crystal Size Distribution in the Case of Agglomeration and Breakage for Batch Cooling Crystallization Process. *Aust. J. Basic & Appl. Sci.*, 11(3): 128-136, 2017

extend the original analytical CSD estimator to cover the effects of agglomeration and breakage phenomena in order to obtain the desired target CSD. The application of the extended analytical CSD estimator is highlighted using sucrose crystallization case study. Here by specifying the target CSD, multiple set-points needed to achieve the target CSD are generated using extended estimator. The closed-loop simulation for sucrose crystallization is then performed for every generated set-point. The final CSDs obtained from every set-point are then compared and discussed.

Research Methodology:

Extension of Analytical CSD Estimator with Agglomeration-Breakage:

Previously, the analytical CSD estimator by Aamir (2010) has been developed under assumptions of constant supersaturation and crystal growth dominant phenomena. The function of this estimator is to generate a supersaturation set-point that provides a target crystal size distribution (CSD) assuming the initial seed distribution and growth kinetics of the system are known. In this work, the original analytical CSD estimator has been extended to cover the effects of agglomeration and breakage to analyze its effect towards the performance of the CSD. Here the agglomeration and breakage is defined as the production-reduction term and represented by the expressions term as shown in the Eqn. 1 below (Quintana-hernandez *et al.*, 2004).

$$\alpha(L) = K_a S^a M_c^k N_{rpm}^l \quad (1)$$

In addition the effects of agitation rate are also considered in the extended analytical CSD estimator. Population balance equation (f_n) incorporating production-reduction term, $\alpha(L)$ for one-dimensional case is shown in Eqn. 2.

$$\frac{df_n(L_{x,i}, t)}{dt} + \frac{dG_x(L_{x,i}, t) df_n(L_{x,i}, t)}{dL_{x,i}} = \alpha(L) \quad (2)$$

Where L_x is the characteristic length of crystal particles.

In the case of size independent growth rate (G_x), Eqn. (2) can be rewritten as:

$$\frac{df_n}{dt} + G_x \frac{df_n}{dL_{x,i}} = \alpha(L) \quad (3)$$

The expression for size independent growth is given by:

$$G_x = K_{gx} S^{gx} N_{rpm}^q \quad (4)$$

where K_{gx} is kinetic coefficient of crystal growth
 S is relative supersaturation of crystal growth
 N_{rpm} is agitation rate

The supersaturation is assumed to be constant which is possible in a controlled crystallization and supersaturation expression is given by:

$$S = \frac{c - c^{sat}}{c^{sat}} \quad (5)$$

where c is initial concentration
 c^{sat} is saturation concentration

Differentiating Eqn. (4) with respect to characteristic length gives:

$$\frac{dG_x}{dL_x} = 0 \quad (6)$$

Introduce $f_n(L_{x,i}, t) = f_n(L_{x,i}(Z), t(Z))$ and by applying chain rule give:

$$\frac{dL_{x,i}}{dZ} \frac{df_n}{dL_{x,i}} + \frac{dt}{dZ} \frac{df_n}{dt} = \frac{df_n}{dZ} \quad (7)$$

Comparing Eqn. (7) and (3) give:

$$\frac{dt}{dZ} = 1 \quad (8)$$

$$\frac{dL_{x,i}}{dZ} = G_x \quad (9)$$

$$\frac{df_{n,i}}{dZ} = \alpha \quad (10)$$

Integrating Eqn. (8) with limits:

$$(t - t_0) = (Z - Z_0) \quad (11)$$

By assuming $t_0 = Z_0 = 0$, Eqn. (11) can be simplified:

$$t = Z \quad (12)$$

Since $dt = dZ$, Eqn. (9) becomes:

$$\frac{dL_{x,i}}{dt} = G_x \quad (13)$$

Substitute Eqn. (4) into (13) gives:

$$\frac{dL_{x,i}}{dt} = K_{gx} S^{gx} N_{rpm}^q \quad (14)$$

Integrating Eqn. (14) with limits:

$$(L_{x,i} - L_{x0,i}) = K_{gx} S^{gx} N_{rpm}^q (t - t_0) \quad (15)$$

By assuming $t_0 = 0$, Eqn. (15) can be simplified:

$$(L_{x,i} - L_{x0,i}) = K_{gx} S^{gx} N_{rpm}^q t_c \quad (16)$$

Rearranging Eqn. (16) gives:

$$L_{x,i} = L_{x0,i} + K_{gx} S^{gx} N_{rpm}^q t_c \quad (17)$$

Since $dt = dZ$, thus:

$$\frac{df_{n,i}}{dt} = \alpha(L) \quad (18)$$

Integrating Eqn. (18) with limit:

$$f_{n,i} = f_{n0,i} + K_a S^a M_c^k N_{rpm}^q \quad (19)$$

The final expressions of the extended analytical CSD estimator are shown in Table 1.

Table 1: Analytical CSD estimator for sucrose

Characteristic	Analytical model equations
Size independent growth : $G = K_g S^g N_{rpm}^q$	Final CSD : $f_{n,i} = f_{n0,i} + K_a S^a M_c^k N_{rpm}^r$, $i = 1, 2, \dots, N$
	Final characteristic length: $L_{x,i} = L_{x0,i} + K_g S^g N_{rpm}^q t_c$, $i = 1, 2, \dots, N$

To generate the optimal supersaturation set-point using the extended analytical CSD estimator, three conditions must be taken into accounts which are the initial seed of crystals, a target CSD and parameters that represent the growth kinetic must be available. Usually, the target CSD, $f_{n,i \text{ target}}$ is specified by the users in the form of normal, lognormal or bimodal distribution (Aamir, 2010). Here in this paper the initial seed distribution of the seeded batch crystallizer is assumed to be a parabolic distribution as reported by Shi *et al.* (2006) that starts from 250 to 300 μm as shown in Eqn. (20). The initial seed of CSD needs to be specified since it serves as a starting point for the crystals starts to grow from initial characteristic length (Samad *et al.*, 2013).

$$n(L,0) = 0.0032(300-L)(L-250) \quad , \text{for } 250\mu\text{m} \leq L \leq 300\mu\text{m}$$

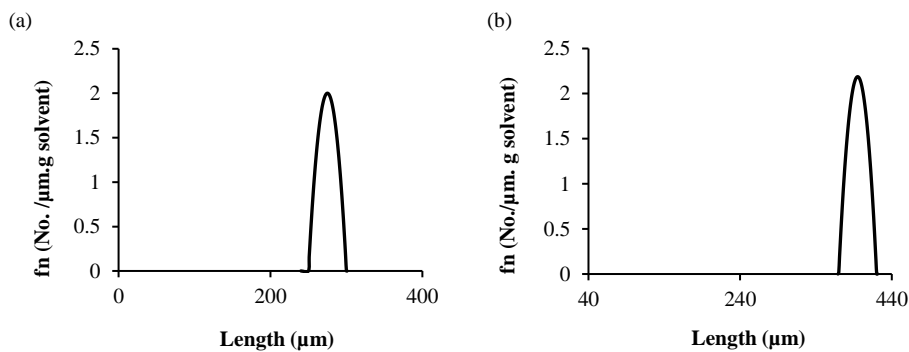
$$n(L,0) = 0 \quad , \text{for } L < 250\mu\text{m} \text{ and } L > 300\mu\text{m} \quad (20)$$

In this study, the target seed distribution chosen is also in the parabolic distribution as shown in the Equation (20).

$$n(L,0) = 0.0035(420-L)(L-370) \quad , \text{for } 370\mu\text{m} \leq L \leq 420\mu\text{m}$$

$$n(L,0) = 0 \quad , \text{for } L < 370\mu\text{m} \text{ and } L > 420\mu\text{m} \quad (21)$$

Figure 1 shows the initial seed of CSD and target CSD generated from Eqns. (20) and (21). The highest peak for the initial seed is 2/ μm . g solvent meanwhile for the target CSD is 2.12/ μm . g solvent. Usually, in the case of size independent growth where the effects of both agglomeration and breakage are neglected, the peak and the curve shape of the initial and final CSD are similar except the mean of the characteristic length is increased due to the growth effect (Samad *et al.*, 2013). However, in this case study with the incorporation of agglomeration and breakage, both the curve shape of CSD and characteristic length are changed.

**Fig. 1:** (a) Initial seed distribution (b) target seed distribution for sucrose crystallization

A model-based approach as shown in Eqns. (22) to (25) is then used to optimize the supersaturation set point and the total crystallization time in order to achieve the desired target CSD. The objective is to minimize the sum of squares of the relative errors between the desired target CSD and a predicted CSD obtained through the extension of analytical CSD estimator.

Minimize

$$F_{obj} = \sum_{i=1}^N \left(\frac{f_{n,i} - f_{n,i \text{ target}}}{f_{n,i \text{ target}}} \right)^2 \quad (22)$$

Subject to: S_{sp}, t_c

$$S_{sp, \min} \leq S_{sp} \leq S_{sp, \max} \quad (23)$$

$$t_{\min} \leq t_c \leq t_{\max} \quad (24)$$

$$C_{t \text{ batch}} \leq C_{f \text{ max}} \quad (25)$$

Where N is the number of discretization points, $f_{n,i}$ is the predicted CSD that is obtained from the analytical CSD estimator and $f_{n,i \text{ target}}$ is the desired target CSD, $c_{t, \text{ batch}}$ is the expected solute concentration at the end of the batch and $c_{f, \text{ max}}$ represents the maximum acceptable solute concentration at the end of the batch to achieve the required yield.

RESULTS AND DISCUSSIONS

Simulation Results:

The case study used to demonstrate the application of the extended analytical CSD estimator is highlighted through sucrose crystallization process which has been adopted from Quintana-hernandez *et al.* (2004). The mathematical model used for sucrose case study is shown in Table 2 which is similar as published in the literature (Quintana-hernandez *et al.*, 2004). The only difference is in this work the population balance equations are solved using the method of classes.

Table 2: List of model equations for the one dimensional model for sucrose (Samad *et al.*, 2013)

Population balance equation (size independent growth)	$\frac{dN_1}{dt} + \frac{G(L_1)}{2\Delta(Cl_2)}N_2 + \frac{G(L_1)-G(L_0)}{2\Delta(Cl_2)}N_1 = B + \alpha, i = 1$
	$\frac{dN_i}{dt} + \frac{G}{2\Delta(Cl_i)}N_i - \frac{G}{2\Delta(Cl_{i-1})}N_{i-1} = \alpha, 1 \leq i \leq n$
	$\frac{dN_n}{dt} + \frac{G}{2\Delta(Cl_n)}N_n - \frac{G}{2\Delta(Cl_{n-1})}N_{n-1} = \alpha, i = n$
Overall mass balance (solute concentration)	$\frac{dc}{dt} = -3\rho_c k_v G \left(\sum_{i=1}^n S_{xi}^3 \frac{dN_i}{dt} \right)$
Energy balance	$\frac{dT}{dt} = -\frac{UA}{M c_p} (T - T_w) - \frac{\Delta H}{c_p} 3\rho_c k_v G \left(\sum_{i=1}^n S_{xi}^3 \frac{dN_i}{dt} \right)$
Energy balance for cooling jacket	$\rho_w V_w c_{pw} \frac{dT_w}{dt} = \rho_w F_{win} c_{pw} (T_{win} - T_w) + U_1 A_1 (T - T_w) + U_2 A_2 (T_{ex} - T_w)$
Saturation concentration	$c^{\text{sat}}(T) = 6.29 \times 10^{-2} + 2.46 \times 10^{-3}T - 7.14 \times 10^{-6}T^2$
Supersaturation	$S = \frac{c - c^{\text{sat}}}{c^{\text{sat}}}$
Nucleation	$B = K_b S^b M_c^j N_{rpm}^p$
Crystal growth rate (length direction)	$G_x = K_g S^g N_{rpm}^q$
Characteristic size	$S_{xi} = \frac{L_{xi} - L_{xi-1}}{2}$
Production reduction-term	$\alpha(L) = K_a S^a M_c^k N_{rpm}^r$
Total crystal mass	$M_c = \rho_c k_v \left(\sum_{i=1}^n S_{xi}^3 N_i \right)$
Crystal size distribution	$f_n(L_{xi}) = \frac{(N_i / \Delta cl_i) + (N_{i+1} / \Delta cl_{i+1})}{2}$

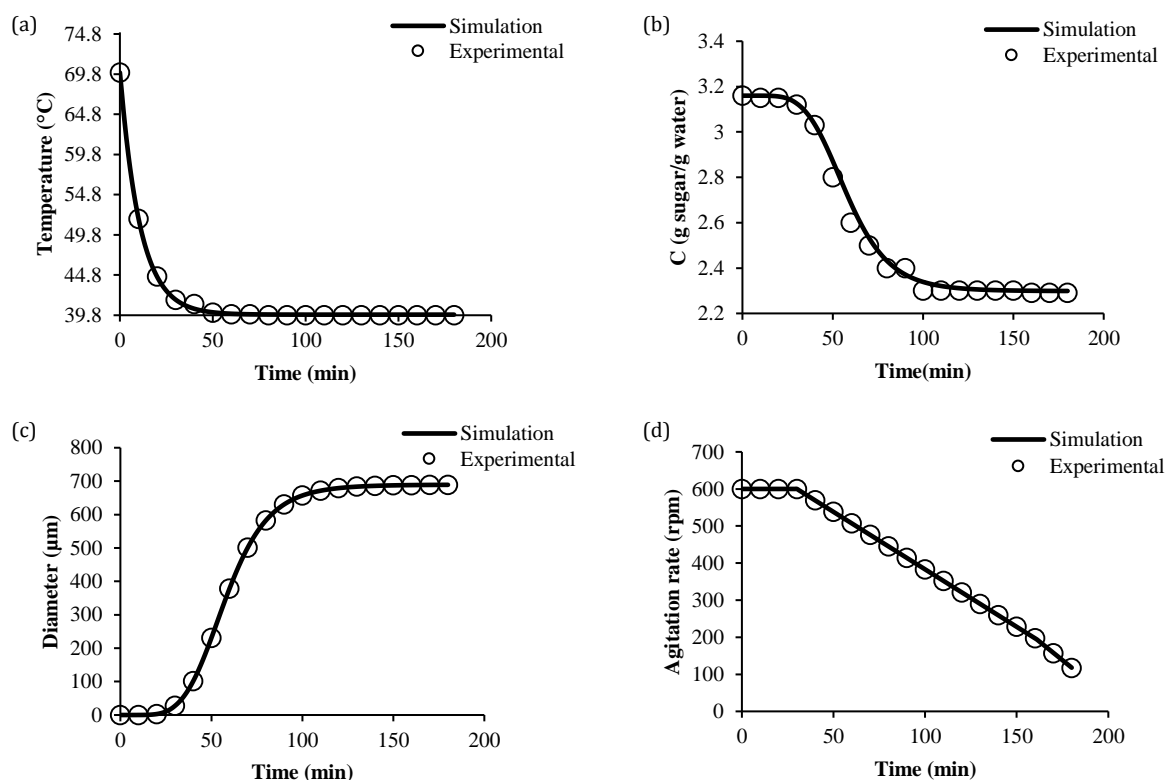
Meanwhile Table 3 shows the values of all parameters and known variables used to solve the mathematical model. In this work the sucrose crystallization mathematical model is developed in Matlab 2014a software and is solved using “ode15s” solver.

Table 3: Parameter values and initial conditions for the sucrose batch cooling crystallizer (Quintana-hernandez *et al.*, 2004)

Parameter	Value	Units
Nucleation order, b	0.01	-
Kinetic coefficient for nucleation, K_b	85.70	No. of particles /cm ³ .min.(g/cm ³) ^j (rpm) ^p
Growth order, g	1.00	-
Kinetic coefficient for crystal growth, K_g	1.33 x 10 ⁻⁴	cm/min.(rpm) ^q
Kinetic coefficient for production-reduction, K_a	1.00	No. of particles /cm ³ .min.(g/cm ³) ^k (rpm) ^r
Production-reduction term, α	0.1	-
Mass order at nucleation, j	5.00 x 10 ⁻³	-
Mass order at production-reduction, k	0.09	-
Agitation order at growth, p	0.05	-
Agitation order at growth, q	0.5	-
Agitation order at production-reduction, r	1.0 x 10 ⁻³	-
Particle shape factor, k_v	$\pi/6$	-
Heat capacity of solution, C_{ps}	2.4687	J/g°C
Density of crystals, ρ_c	1.588	g/cm ³
Density of water, ρ_w	1.0	g/cm ³
Magma volume, V	2230	cm ³
Heat capacity of water, C_{pw}	4.18	J/g°C
Volume of water, V_w	820	cm ³

Exterior temperature, T_{ex}	29	°C
Mass of total, M_T	3328	G
Mass of water, M_w	800	G
Mass of solvent, M_s	2528	G
Mean length, AL	20.2525	μm
Crystal length, L_o	15.126	μm
Cooling water flow rate, F_{win}	8100	cm^3/min
Initial concentration, C	3.16	g sucrose/g water
Initial temperature, T	70	°C
Initial jacket temperature, T_j	70	°C
Initial agitation rate	600	rpm

In this study, the mathematical model for sucrose crystallization process is solved under two conditions. Firstly, under open-loop simulation which will be acted as model validation and secondly under closed-loop simulation where the controller is employed in order to maintain the specified set-point at the desired trajectory. The open-loop simulation results for unseeded sucrose crystallization are shown in Figure 2 for model validation purposes. The crystallization starts with the initial cooling operation where the solution was cooled down from 70°C to reach the saturation concentration. The sucrose concentration initially started at 3.16 g sucrose/g water is saturated at time 4.87 minutes. Once the saturation point is reached, the solution is further cooled to create supersaturation conditions where the solution starts to crystallize. However the concentration still maintained due to most crystal nuclei generated from nucleation kinetic will dissolve back to the solution and only starting to decrease obviously at time 43.4 minutes. The crystal nuclei then start to grow, thus necessitating the crystal growth rate kinetic until the end of the operation. The temperature profile when cooling down from 70 to 40°C based on the natural cooling and a concentration of 2.33 g sucrose/g water was achieved by the end of the process as shown in Figure 2. Here approximately 460 g of the total crystal mass and 670 μm of mean size diameter were obtained based on the open-loop simulation. Here both total crystal mass and mean size diameter were obtained from crystal particles where it has been generated from nucleation kinetic since this is the unseeded system. Based on the simulation results of temperature, concentration, mean size diameter, agitation rate, supersaturation and total crystal mass profile, it shows that both simulation and experimental data are in good agreement indicating thereby a reliable and validated model are achieved.



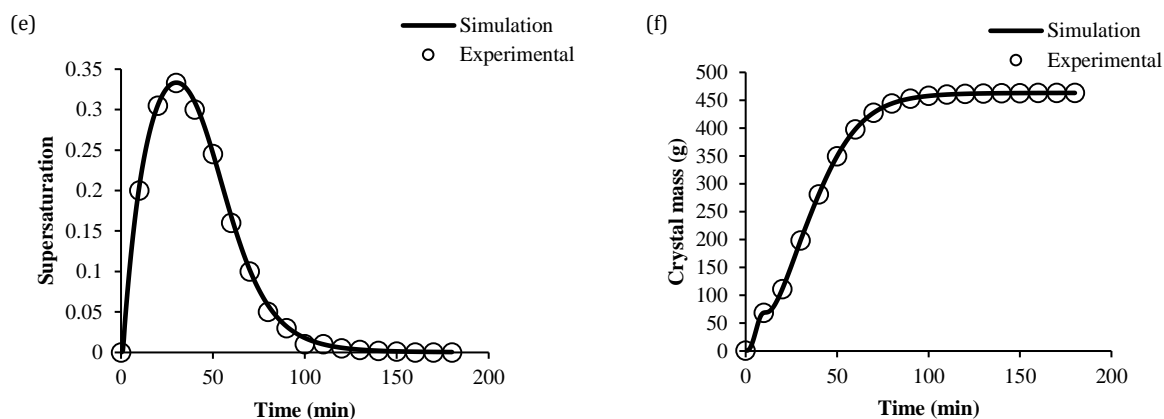


Fig. 2: (a) Temperature (b) Concentration (c) Mean size diameter (d) Agitation rate (e) Supersaturation (f) Total crystal mass profile of sugar in water

The next step concerns on the closed-loop simulation where controller performance is evaluated for maintaining the set-point at its trajectory. For this purpose, the extended analytical CSD estimator is employed by using the initial seed of CSD and target CSD as shown in Figure 1. The set-points generated from the model-based approach (Eqns. (22) to (25)) are shown in Table 4. All of the generated set-points will be tested in the closed-loop simulation to achieve the desired target CSD if it is maintained in the specified trajectory. For the closed-loop simulation, a proportional integral (PI) controller has been considered to maintain the sucrose concentration at the desired set-point.

Table 4: Supersaturation set-point values for the seeded sucrose batch cooling crystallizer

Time (min)	Supersaturation set-point (g/g)
150	0.0352
180	0.0312
210	0.0281

The closed-loop simulation results obtained are shown in Figure 3. The sucrose concentration profiles for all closed-loop simulation were successfully maintained at the required set-point until the end of the operation indicating a reliable PI controller. The sucrose concentration initially at 3.12 g sucrose/g water is decreased steadily to 2.30 g sucrose/g water at the end of operation time of 150 minutes, 180 minutes, and 210 minutes respectively. Meanwhile Figure 4 shows the temperature profiles when cooling down from 67 °C to 40 °C. It can be observed that the concentration is depending on the temperature where the concentration is decreased when the temperature is also decreased.

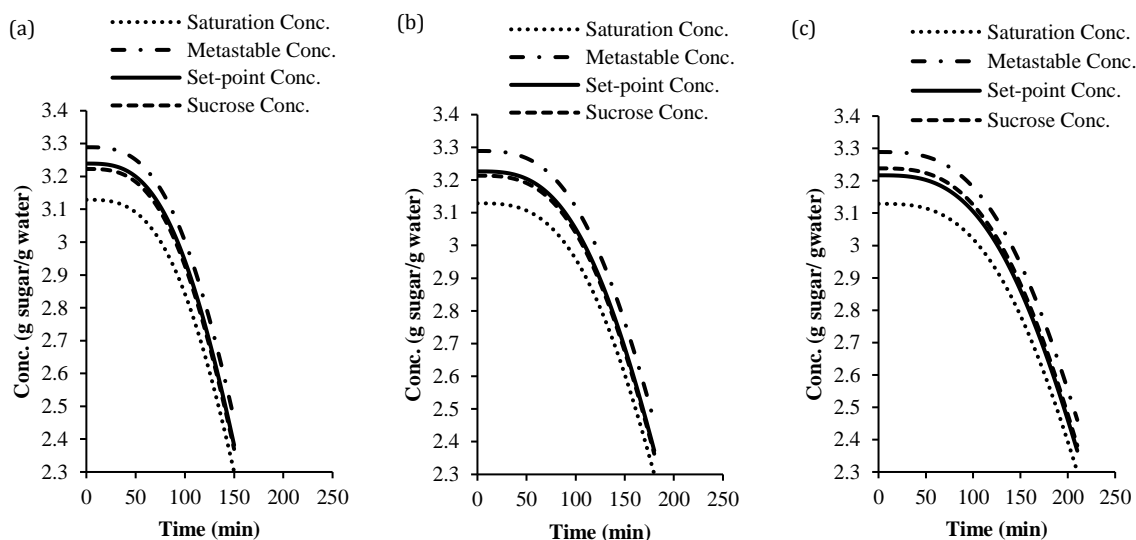


Fig. 3: (a) Concentration profile of sugar in water at 150 min (b) 180 min (c) 210 min.

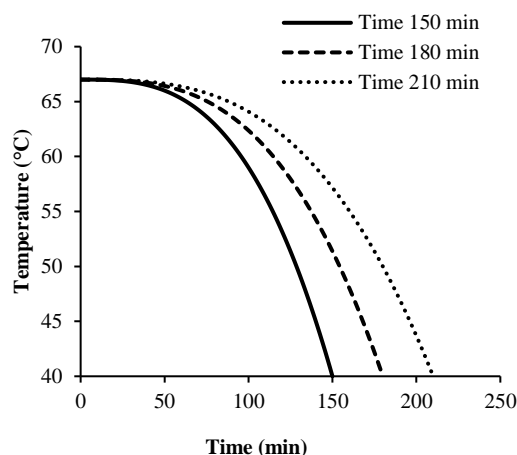


Fig. 4: Temperature profiles of sucrose crystallization

Meanwhile Figure 5 shows the mean size diameter and crystal size distribution for the sucrose crystallization process. The initial mean size diameter for seed crystals is $275 \mu\text{m}$ and the mean size is increased to $614 \mu\text{m}$ at the end of operation for all set-points as shown in Figure 5(a). This is due to the sucrose in the solution has been transferred into a seed crystal and thus resulting into the increment of the mean size diameter. Figure 5(b) shows the initial seed and final CSD for sucrose crystallization process. When the agglomeration-breakage is incorporated, the sucrose crystallization resulted in final crystal size distribution (CSD) at 210 minutes is about $2.12 \mu\text{m}$ per gram of solvent, with an approximate mean of $395 \mu\text{m}$ as similar to the targeted distribution. At this phase, the seeded formation for final CSD are tends to agglomerate rather than breakage due to the higher crystal size distribution value obtained. However, the secondary peak is appeared in the final CSD due to the nucleation effects that cannot be captured by the analytical estimator. As shown in Figure 5(b), the highest secondary peak was obtained when operating the crystallization process for 150 minutes (supersaturation set-point of 0.0352). Although the target CSD was achieved when operating at this condition however the drawback is higher secondary peak was obtained. This is due to the supersaturation set-point at 0.0352 operated closer to the metastable limit and thus more secondary nucleation has occurred in the operation. The secondary nucleation is not favorable in the crystallization process because it will produces more crystal particles at lower characteristic length and will affecting the growth of crystal seed. Meanwhile supersaturation set-point of 0.0281 and total crystallization time of 210 minutes produce lower secondary peak but the total crystallization time for this operation is too long compared to the others. This is mainly because the crystallizer has been operated close to the saturation line, and under such conditions it will take a long time to achieve the target CSD. If the total crystallization time is taken into consideration then it will not be very practical since the operating costs typically increase the longer the batch runs. As an alternative set-point of 0.0321 at crystallization time of 180 minutes can be selected due to its reasonable operation time while the performance is still acceptable, producing a CSD that is close to the target CSD generated by the analytical CSD estimator.

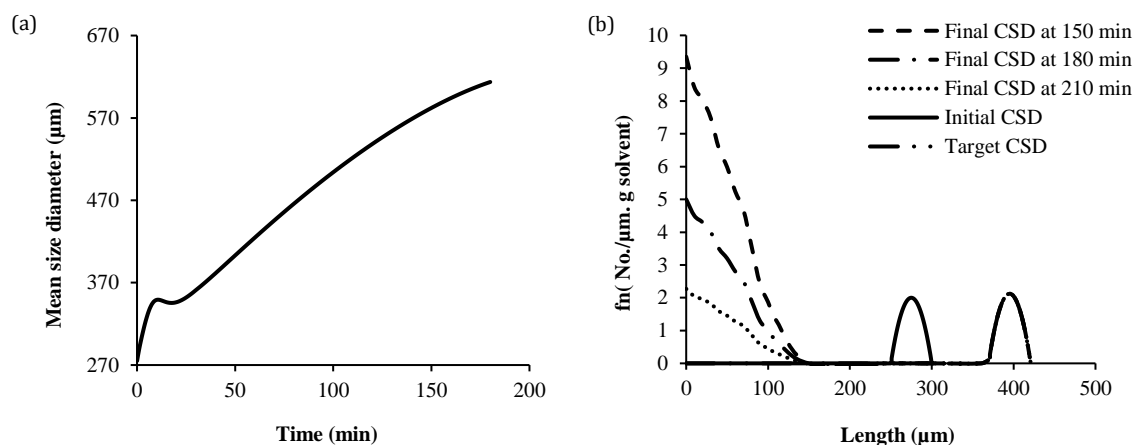


Fig. 5: (a) Mean size diameter (b) Crystal size distribution (CSD) for sucrose

Conclusion:

An analytical CSD estimator has been extended to determine the set-point trajectory for all the necessary phenomena (crystal growth, agglomeration and breakage). Sucrose in batch crystallization process was considered as a case study. Based on the closed-loop simulation results, the extended analytical CSD estimator is able to provide the accurate supersaturation set-point in achieving the desired target CSD in the case of agglomeration and breakage phenomena. Although the target CSD is achieved using multiple set-points, however it is important to note that the shorter crystallization time yields a high secondary peak and a tradeoff needs to be decided between operational time and fines crystal production from secondary nucleation.

ACKNOWLEDGEMENT

The financial support for this Master project provided by the Universiti Malaysia Pahang (UMP) Vot Number RDU140395 is gratefully acknowledged.

REFERENCES

Aamir, E., 2010. Population balance model-based optimal control of batch crystallization processes for systematic crystal size distribution design, PhD thesis, Department of Chemical Engineering, Loughborough University, United Kingdom.

Nagy, Z.K., E. Aamir, 2012. Systematic design of supersaturation controlled crystallization processes for shaping the crystal size distribution using an analytical estimator, *Chemical Engineering Science*, 84: 656-670.

Quintana-Hernandez, P., E. Bolanos-Reynoso, B. Miranda-Castro, L. Salcedo-Estrada, 2004. Mathematical modelling and kinetic parameter estimation in batch crystallization, *American Institute of Chemical Engineers*, 50(7): 1407-1417.

Paengjuntuek, W., P. Kittisupakorn, A. Arpornwichanop, 2008. On-line dynamic optimization integrated with generic model control of a batch crystallizer, *Journal of Industrial and Engineering Chemistry*, 14: 442-448.

Samad, N.A.F.A., G. Sin, K.V. Gernaey, R. Gani, 2013. A systematic framework for design of process monitoring and control (PAT) systems for crystallization processes, *Computers and Chemical Engineering*, 54: 8-23.

Shi, D., N.H. El-Farra, M. Li, P. Mhaskar, P.D. Christofides, 2006. Predictive control of particle size distribution in particulate processes, *Chemical Engineering Science*, 61: 268-281.